Politecnico di Milano
Department of Structural Engineering

Non linear viscoelastic model in the spectral element code GeoELSE

Laura Scandella

December 2007

Table of contents

Non-linear viscoelastic model in the Spectral Element code GeoELSE

1 The non-linear viscoelastic model

The adopted non-linearity implies that at each time step of the analysis the Young modulus and the viscous damping are updated on the basis of the maximum deformation achieved at each element of the model. In particular, referring to the 2D Mohr circle (see figure 1.1), the maximum shear deformation γ_{max} is evaluated at each LGL node from the principal strains e_I and e_{II} , solution of the following 2D eigenvalue problem:

$$\boldsymbol{\varepsilon}\mathbf{n}_\alpha = \boldsymbol{e}\mathbf{n}_\alpha$$

$$\begin{bmatrix} \varepsilon_x - e & \frac{1}{2}\gamma_{xy} \\ \frac{1}{2}\gamma_{yx} & \varepsilon_y - e \end{bmatrix} \begin{Bmatrix} n_x \\ n_y \end{Bmatrix} = \begin{Bmatrix} 0 \\ 0 \end{Bmatrix}. \tag{1.1}$$

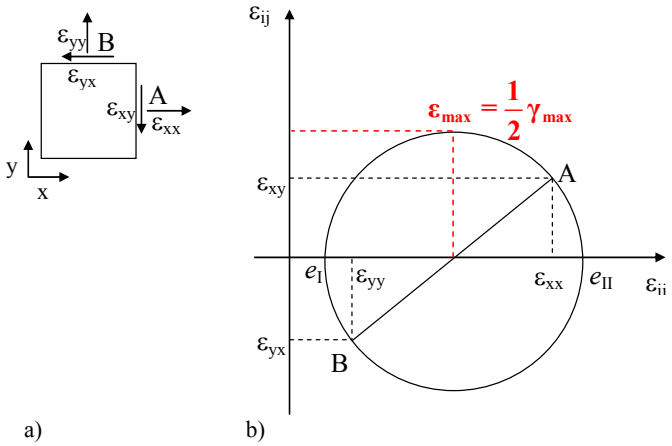

Fig. 1.1 – 2D Mohr circle (b) with the principal strains e_I and e_{II} and the highlighted maximum shear strain ε_{max}, due to the strain field on an infinitesimal element (a)

The eigenvectors (principal strains) are the solutions of the second order equation:

$$\det(\boldsymbol{\varepsilon} - \boldsymbol{e}) = e^2 - I_1 e + I_2 = 0\,, \tag{1.2}$$

with I_1 and I_2 the deformation invariants:

$$\begin{aligned} I_1 &= \varepsilon_x + \varepsilon_y \\ I_2 &= \varepsilon_x \varepsilon_y - \frac{1}{4}\gamma_{xy}\gamma_{yx} \end{aligned}\,. \tag{1.3}$$

e_I and e_{II} are:

$$e_{I,II} = \frac{I_1}{2} \pm \sqrt{\left(\frac{I_1}{2}\right)^2 - I_2}\,. \tag{1.4}$$

The maximum shear strain ε_{max} equals the radius of the Mohr circle, as shown in figure 1.1, namely:

$$\frac{e_{II} - e_I}{2} = 2\sqrt{\left(\frac{I_1}{2}\right)^2 - I_2}\,. \tag{1.5}$$

It follows that $\gamma_{max} = 2 \cdot \varepsilon_{max}$ becomes:

$$\gamma_{\max} = \sqrt{\left(\frac{1}{2}\left(\varepsilon_x - \varepsilon_y\right)\right)^2 + \left(\frac{1}{2}\gamma_{xy}\right)^2} = \sqrt{\left(\frac{1}{2}\left(\frac{\partial u_x}{\partial x} - \frac{\partial u_y}{\partial y}\right)\right)^2 + \left(\frac{1}{2}\left(\frac{\partial u_x}{\partial y} + \frac{\partial u_y}{\partial x}\right)\right)^2}\,. \tag{1.6}$$

This value, averaged on each SE element, defines update Young modulus G and damping ratio ζ at each time step, following a material stress-strain and a damping-strain curve respectively. For instance, in the following validations the curves proposed by Seed & Idriss (1970) shown in figure 1.2 for sand and clay respectively are used.

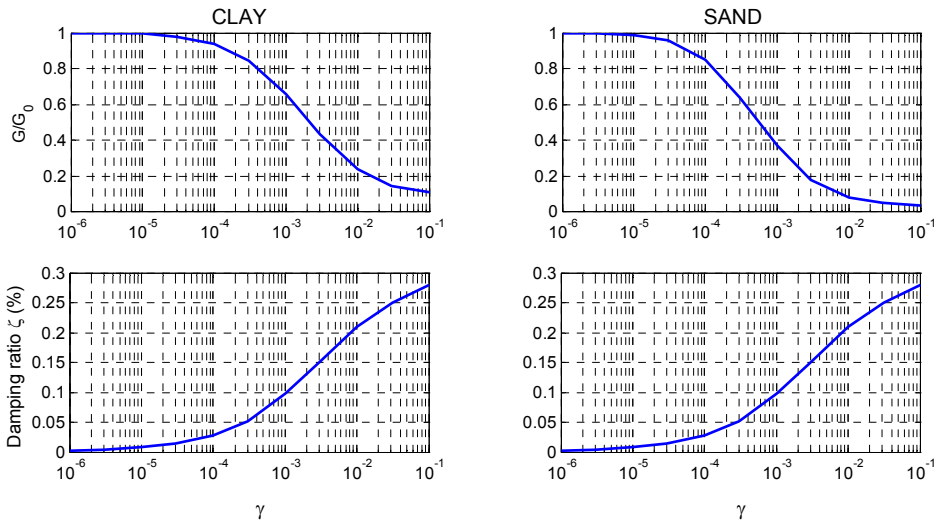

Fig. 1.2 – Example of stress-strain and damping-strain curves: Young modulus degradation (G/G_0) for sand and clay proposed by Seed & Idriss (1970) (above); damping increment (ζ) proposed by Idriss (1990) (below)

An updated shear wave velocity V_S is evaluated assuming constant density ρ_0 in time:

$$V_S = \sqrt{\frac{G}{\rho_0}}\,, \tag{1.7}$$

and a compressional wave velocity V_P is evaluated assuming a constant ratio V_P/V_S. As a consequence the Lamè constant λ can be updated as $\lambda = \rho_0 V_P^2 - 2G$.

Concerning the damping, a damping ratio ζ is evaluated from the Idriss curve shown in figure 1.2 on the base of $\gamma_{max.}$ An updated quality factor is evaluated as:

$$Q = \frac{1}{2\zeta} \tag{1.8}$$

and a damping coefficient $\hat{\gamma}$ as

$$\hat{\gamma} = \frac{\pi f_p}{Q}\,, \tag{1.9}$$

where f_p is the peak frequency which characterize the signal. f_p can be assumed as the peak frequency value of the input velocity time history.

2 Validations

To validate the non-linear viscoelastic model implemented in the SE code GeoELSE, a set of 1D analyses have been performed and the results compared with the seismic response obtained by the analytical code EERA (2000) (Equivalent –linear Earthquake site Response Analyses).

2.1 1D problem

The 1D system adopted for the validations is the layer on a halfspace shown in figure 2.1, characterized by the properties listed in table 2.1. The model has been discretized by spectral elements as a column of elements 10 m large and with an increasing height with depth (10 m in the surface layer). In the numerical model (used by GeoELSE) the halfspace has been limited at the bottom at 1786 m depth. Dirichlet point conditions have been applied at the lateral boundaries to let free only the excited degree of freedom: roller supports which allow the translation in the vertical direction (DIRY) or in the horizontal one (DIRX) when a shear wave or a compressional wave is impinging respectively.

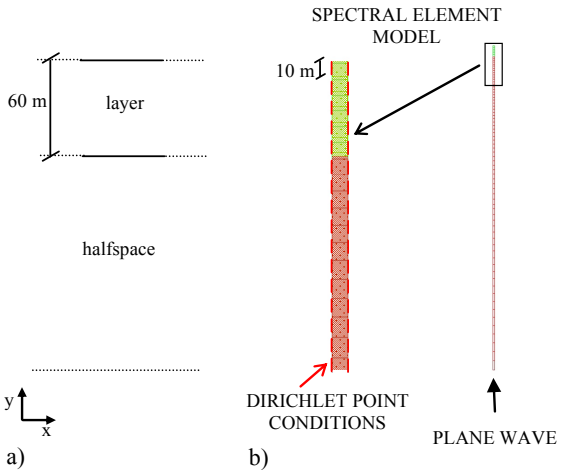

Fig. 2.1 – 1D model of a layer on a halfspace. a): model analysed by EERA; b): numerical model discretized by spectral elements studied by GeoELSE

Tab. 2.1 – Mechanical properties of the 1D model of figure 2.1

a) V_S [m/s]	**b) V_P [m/s]**	**c) ρ [kg/m3]**	**d) G [Pa]**	**e) Q**
f) 100	g) 200	h) 2000	i) 2.00E+7	j) 50
k) 500	l) 1000	m) 2500	n) 6.25E+8	o) 100

Vertically propagating plane waves have been applied as input motion at the base of the model (1761 m depth) in terms of both shear waves and compressional waves. In particular Ricker wavelets with various amplitudes (0.1 mm, 1 mm, 1 cm, 10 cm) and peak frequencies (1 Hz, 0.4 Hz, 0.2 Hz) have been used, as shown in figure 2.2.

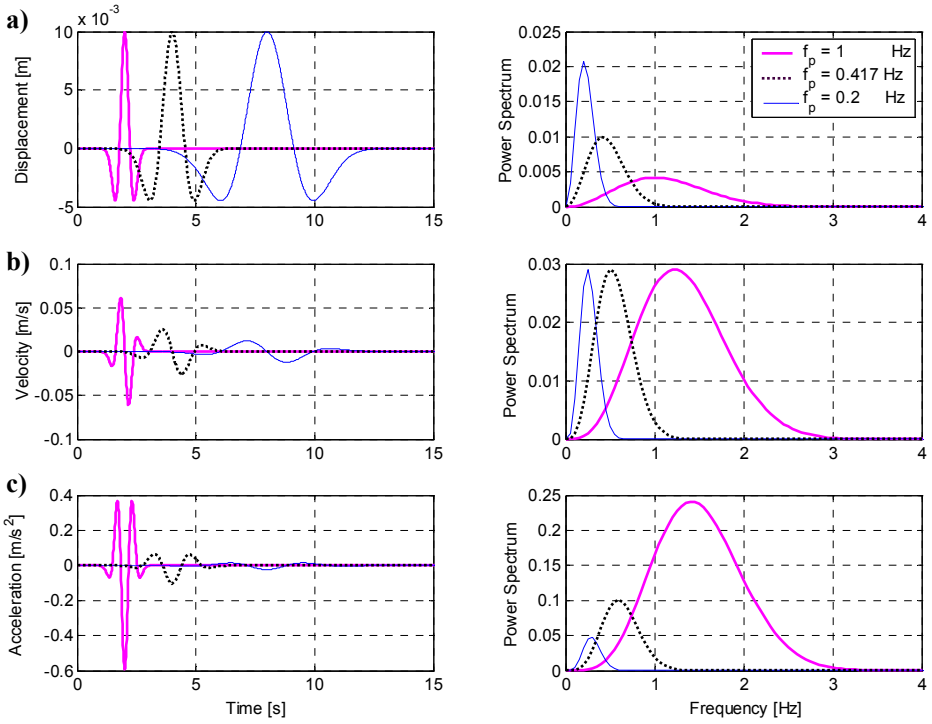

Fig. 2.2 – Input motion: a) Ricker wavelet with 1 cm of amplitude and various peak frequencies (1 Hz (bold lines), 0.417 Hz (dotted lines), 0.2 Hz (thin lines)) as displacement input; b) velocity input; c) acceleration input

Note that f_p = 0.417 Hz is the resonant frequency of the layer (β /4H).

2.2 Input files for GeoELSE

Referring to the 1D problem previously described, a non-linear viscoelastic analysis requires in the input file ***nomefile.mat*** additional information with respect to a linear analysis, as highlighted in figure 2.3.

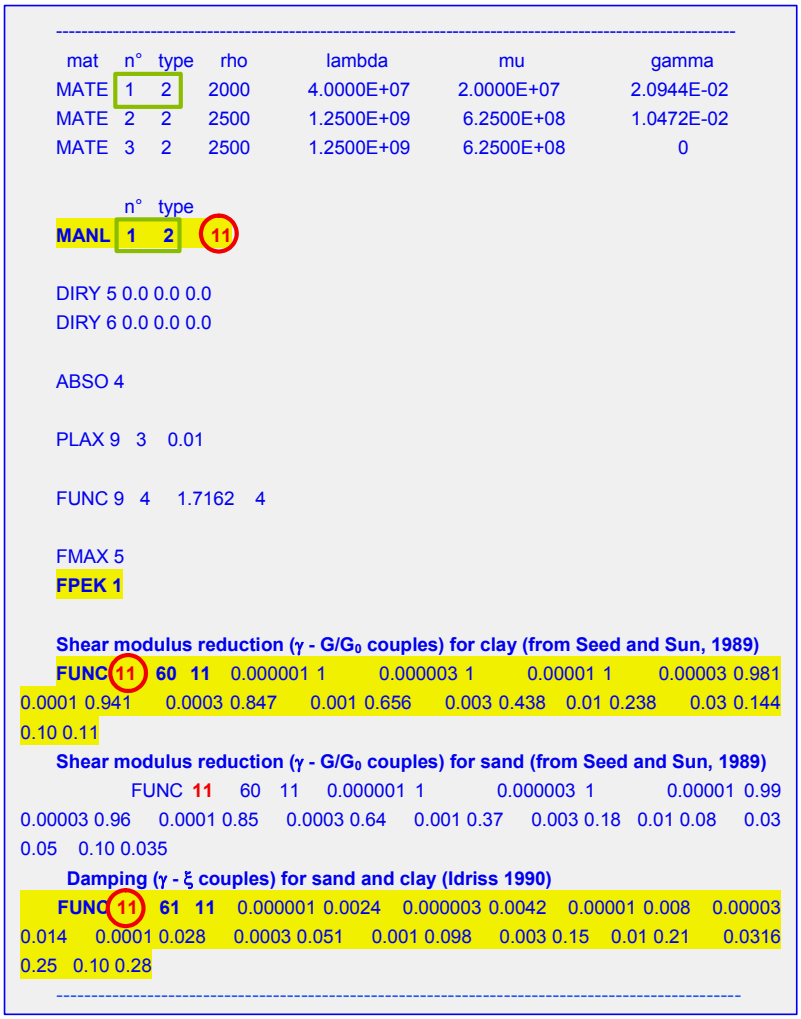

```
---------------------------------------------------------------------------------------------------
 mat   n°  type   rho        lambda          mu            gamma
MATE  1    2     2000     4.0000E+07     2.0000E+07     2.0944E-02
MATE  2    2     2500     1.2500E+09     6.2500E+08     1.0472E-02
MATE  3    2     2500     1.2500E+09     6.2500E+08     0

        n°  type
MANL  1    2     11

DIRY 5 0.0 0.0 0.0
DIRY 6 0.0 0.0 0.0

ABSO 4

PLAX 9   3    0.01

FUNC 9   4    1.7162   4

FMAX 5
FPEK 1

Shear modulus reduction (γ - G/G0 couples) for clay (from Seed and Sun, 1989)
FUNC 11   60   11   0.000001 1      0.000003 1      0.00001 1      0.00003 0.981
0.0001 0.941    0.0003 0.847    0.001 0.656    0.003 0.438    0.01 0.238    0.03 0.144
0.10 0.11
Shear modulus reduction (γ - G/G0 couples) for sand (from Seed and Sun, 1989)
          FUNC 11    60   11    0.000001 1          0.000003 1          0.00001 0.99
0.00003 0.96    0.0001 0.85    0.0003 0.64    0.001 0.37    0.003 0.18   0.01 0.08    0.03
0.05    0.10 0.035
Damping (γ - ξ couples) for sand and clay (Idriss 1990)
FUNC 11   61   11   0.000001 0.0024   0.000003 0.0042   0.00001 0.008   0.00003
0.014    0.0001 0.028    0.0003 0.051    0.001 0.098    0.003 0.15    0.01 0.21    0.0316
0.25   0.10 0.28
---------------------------------------------------------------------------------------------------
```

Fig. 2.3 – Example of "*nomefile.mat*" file referring to the 1D problem described in section 2.1

MANL 1 2 11 means that the material n° **1** of type **2**, whose properties are listed before (green rectangle), is a a non-linear viscoelastic material, following the material stress-strain and damping-strain curves described by function **11**. Various non-linear material can be specified, one at each line.

FUNC 11 60 11 describes the stress-strain curve followed by the MANL (red circle). Function **11** is of type **60** and characterized by the following **11** γ–G/G_0 couples (e.g. figure 1.2,).

FUNC 11 61 11 describes the damping-strain curve followed by the MANL (red circle). Function **11** is of type **61** and characterized by the following **11** γ–ζ couples (e.g figure 1.2).

FPEK 1 specifies the peak frequency f_p of the signal, used for the damping coefficient definition (eq. 1.9)

The other two input files for GeoELSE ***nomefile.inp*** and ***else2_input.d*** are the same as for a linear analysis.

2.3 Output files from GeoELSE

In addition to the output files required in the OPTIOUT for a linear analysis, in the non-linear case, the files

monitorxxxx.g are automatically saved at each receiver:

NON-LINEAR INFORMATION ***monitorxxxx.g*** **| Δt | γ_{max} | *G/G₀* |**

2.4 Comparison between analytical (by EERA) and numerical (by GeoELSE) results

The seismic responses evaluated by an analytical approach (EERA) and the numerical SE method (GeoELSE) are compared in the following. Both the linear and the non-linear viscoelastic behaviour, due to vertically propagating shear plane waves as input motion, have been studied. To simulate 1D vertically incident shear waves (PLAX) with GeoELSE, Dirichlet point conditions are imposed at the lateral boundaries, namely roller supports blocking the translation in the vertical direction (DIRY).

Note that, EERA program calculates the horizontal component of the motion (in terms of displacement, velocity and acceleration) and the shear component of stress and strain only (τ_{xy} and γ_{xy} respectively).

2.4.1 Linear viscoelastic behaviour

The results obtained at the representative depth of 30 m, using a Ricker wavelet with 1 cm of amplitude, and peak frequency of 1 Hz as input motion, are shown.

A good agreement is obtained between the linear seismic response evaluated by EERA and GeoELSE, as shown in figures 2.4 and 2.5. As expected, the shear modulus G remains constant in time and the hysteretic stress-strain cycles (τ_{xy} vs. γ_{xy} diagram) are straight lines, as shown in figure 2.6.

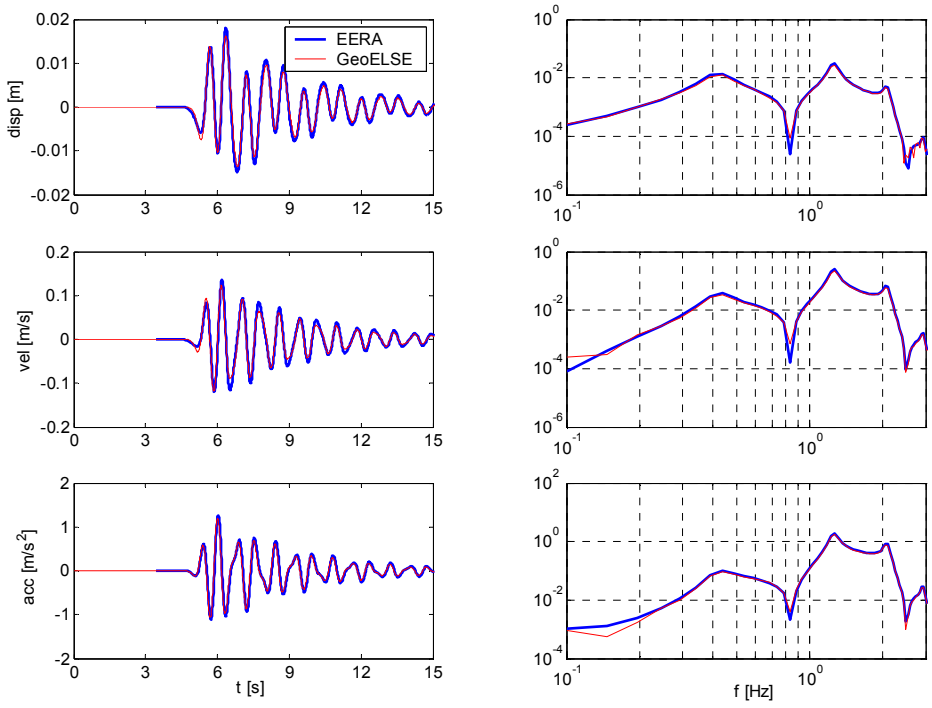

Fig. 2.4 – Comparison between the horizontal seismic responses evaluated in **linear viscoelastic** conditions by EERA (bold line) and GeoELSE (thin line). Time histories (left) and Fourier spectra (right) of displacement, velocity and acceleration in the horizontal direction at the representative depth of 30 m (at the middle of the layer) are shown. The seismic input is a Ricker wavelet of amplitude A= 1 cm and f_p=1 Hz, applied as vertically propagating shear wave

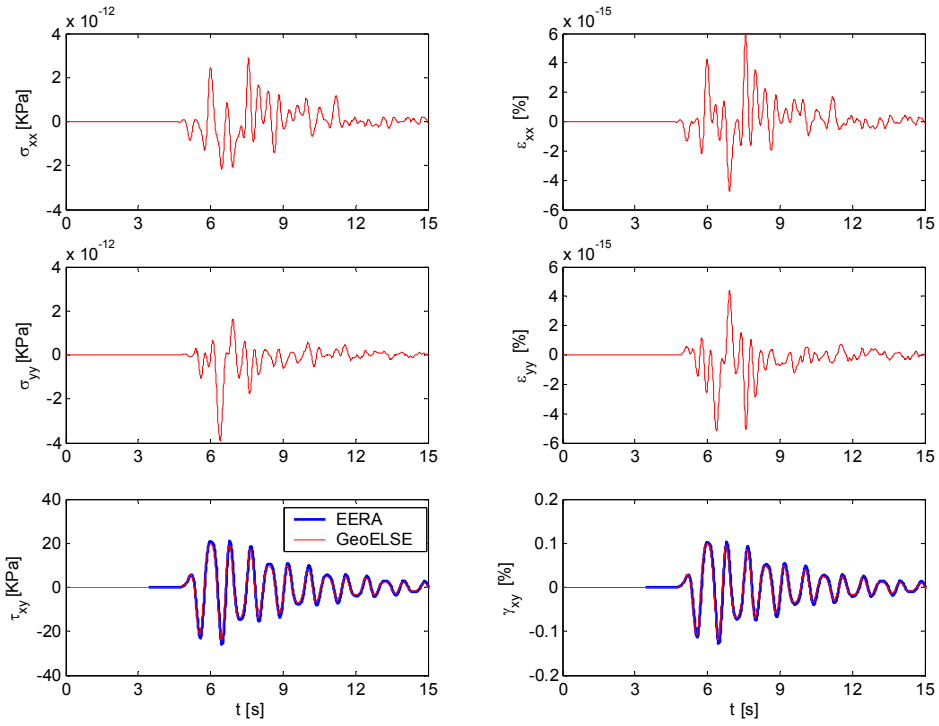

Fig. 2.5 – Comparison between the seismic responses evaluated in **linear viscoelastic** conditions by EERA (bold line) and GeoELSE (thin line). Time histories of stress (left) and strain (right) at the representative depth of 30 m (at the middle of the layer) are shown. The seismic input is a Ricker wavelet of amplitude A= 1 cm and f_p=1 Hz, applied as vertically propagating shear wave

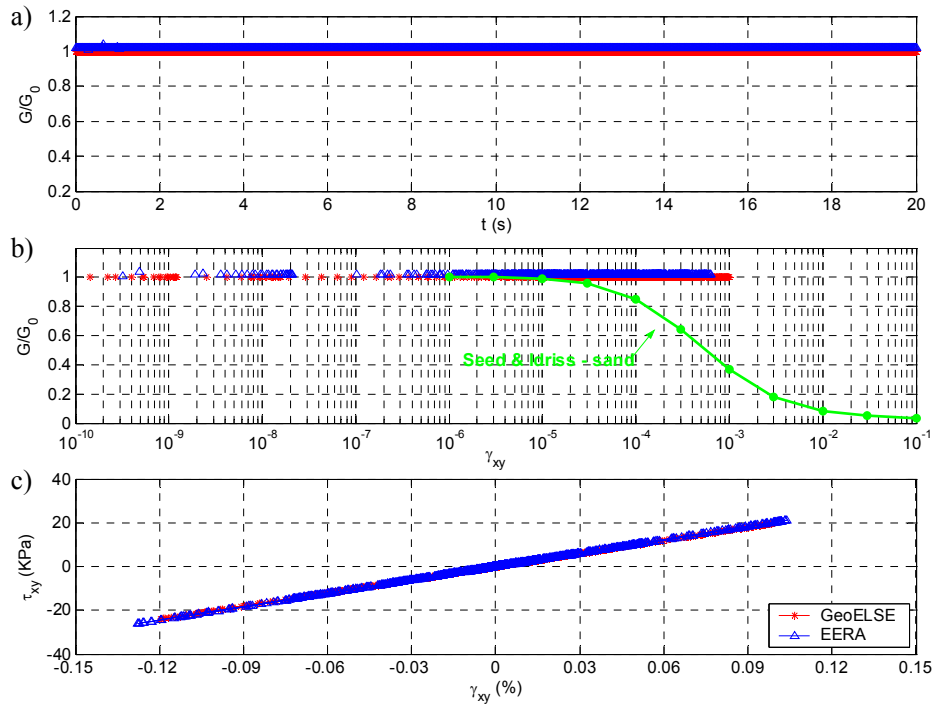

Fig. 2.6 – Comparison between the seismic responses evaluated in **linear viscoelastic** conditions by EERA (triangles) and GeoELSE (stars) at the representative depth of 30 m (in the middle of the layer): a) G/G_o vs. time; b) G/G_o vs. γ_{xy}; c) hysteretic stress-stain cycles. The seismic input is a Ricker wavelet of amplitude A= 1 cm and f_p=1 Hz, applied as vertically propagating shear wave

2.4.2 Non-linear viscoelastic behaviour

The non-linear viscoelastic behaviour of sand has been simulated following the Seed & Idriss (1970) curves shown in figure 1.2. The results obtained at the representative depth of 30 m, using a Ricker wavelet with 1 mm and 1 cm of amplitude, and peak frequency of 1 Hz as input motion, are shown.

A) Input: Ricker wavelet with 1 mm of amplitude and 1 Hz of peak frequency

Using as input motion a Ricker wavelet of amplitude A = 1 mm, the material slightly enter in non-linear field. The seismic response obtained by the equivalent linear model (by EERA, 2000) and the non-linear vicoelastic model (by GeoELSE, as described in section 1), is quite similar, as shown in figures 2.7 and 2.8. In the range of frequencies between 0.8-2 Hz there is a good agreement (figure 2.7), while at low frequencies (< 0.8 Hz) the numerical response is damper and at high frequencies (>2 Hz) it is amplified with respect to the analytical one. This is probably due to the fact that, while the analytical damping is constant in time, in the numerical method it is locally updated in time, so that higher frequencies are less damped. This behaviour is more evident for a higher amplitude of the input motion, as shown in the following.

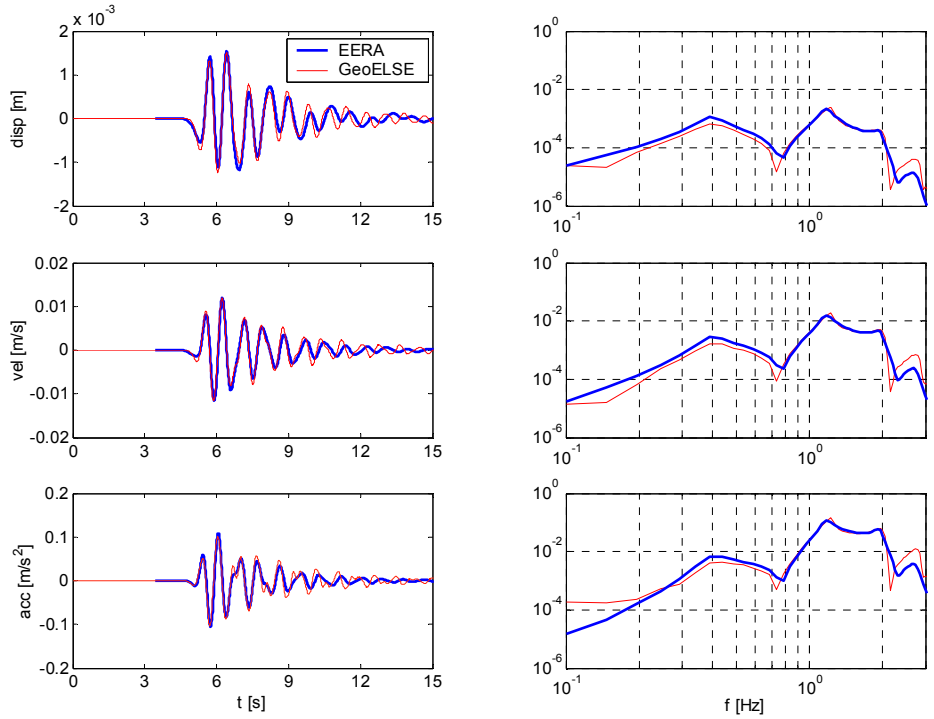

Fig. 2.7 – Comparison between the horizontal seismic responses evaluated in **non-linear viscoelastic** conditions by EERA (bold line) and GeoELSE (thin line). Time histories (left) and Fourier spectra (right) of displacement, velocity and acceleration in the horizontal direction at the representative depth of 30 m (at the middle of the layer) are shown. The seismic input is a Ricker wavelet of amplitude A= 1 mm and f_p=1 Hz, applied as vertically propagating shear wave

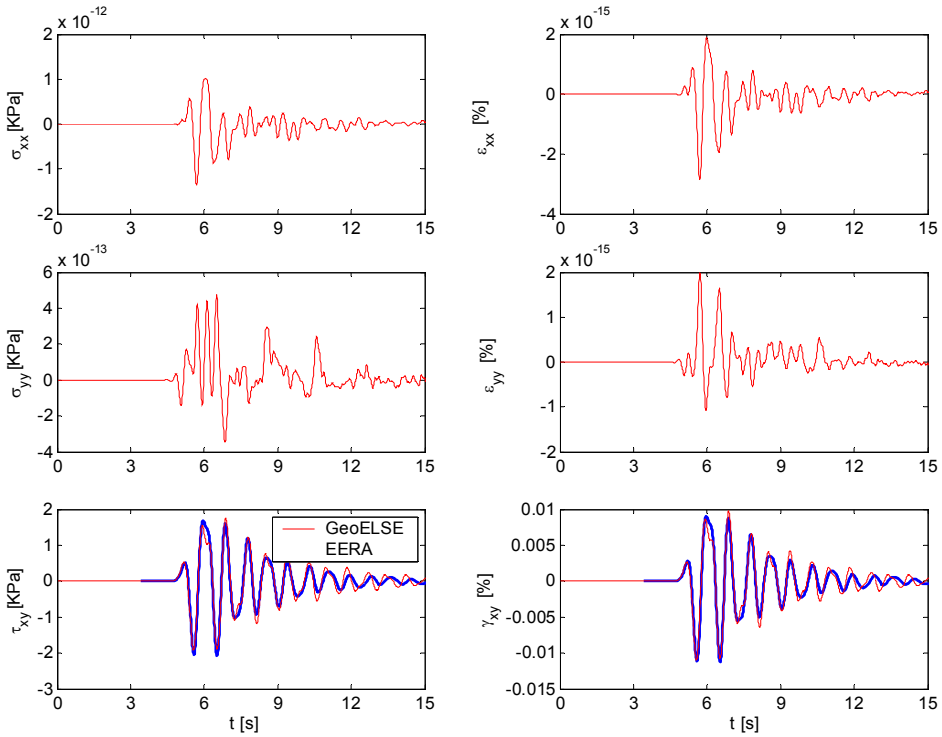

Fig. 2.8 – Comparison between the seismic responses evaluated in **non-linear viscoelastic** conditions by EERA (bold line) and GeoELSE (thin line). Time histories of stress (left) and strain (right) at the representative depth of 30 m (at the middle of the layer) are shown. The seismic input is a Ricker wavelet of amplitude A= 1 mm and f_p=1 Hz, applied as vertically propagating shear wave

The G/G_0 ratios updated in time by GeoELSE are high, in the range 0.85-1, while EERA, at the convergence of the linear equivalent procedure, uses a constant value in time of 0.90 (figure 2.9). The hysteretic cycles are almost aligned along a straight line (figure 2.10). The numerical material behaviour seems to dissipate less energy than the analytical one, being the cycles tighter.

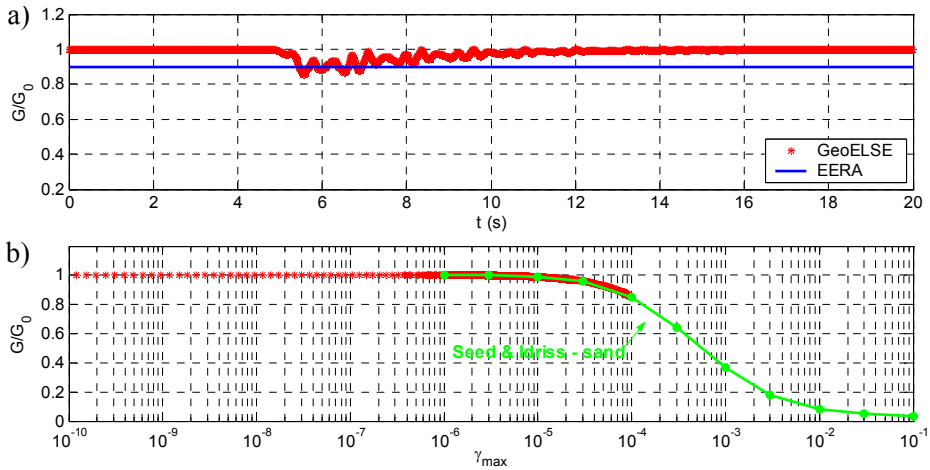

Fig. 2.9 – Seismic response calculated in **non-linear viscoelastic** conditions by GeoELSE (stars) and EERA (line) at the representative depth of 30 m (in the middle of the layer): a) G/G_o vs. time; b) G/G_o vs. γ_{max}. The seismic input is a Ricker wavelet of amplitude A= 1 mm and f_p=1 Hz, applied as vertically propagating shear wave

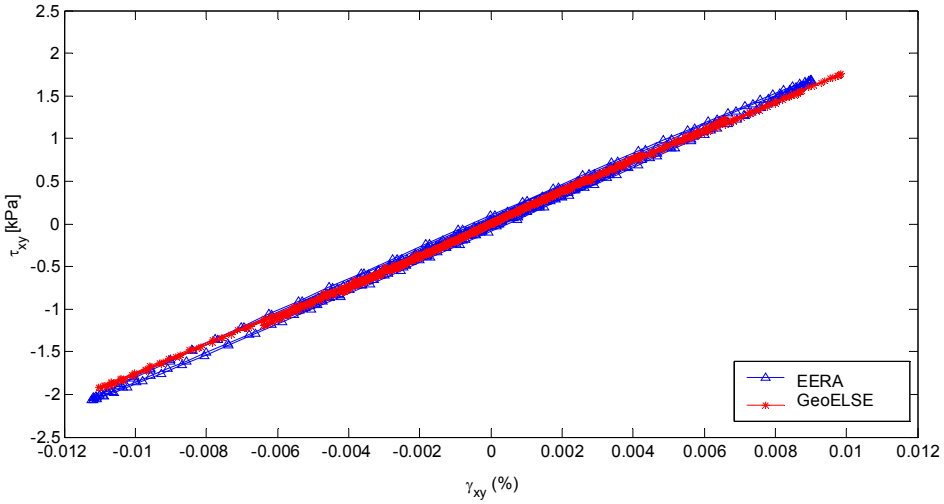

Fig. 2.10 – Comparison between the hysteretic stress-stain cycles evaluated in **non-linear viscoelastic** conditions by EERA (triangles) and GeoELSE (stars) at the representative depth of 30 m (in the middle of the layer). The seismic input is a Ricker wavelet of amplitude A= 1 mm and f_p=1 Hz, applied as vertically propagating shear wave

B) Input: Ricker wavelet with 1 cm of amplitude and 1 Hz of peak frequency

It is important to note that EERA code uses a ratio between the effective γ_{eff} and the maximum shear strain γ_{max} to calculate the convergent equivalent shear modulus degradation. Generally, a ratio $\gamma_{eff}/\gamma_{max}$ of 0.5 is applied to take into account an average value of the modulus degradation in time. In the following, the results obtained using 0.5 γ_{max} and γ_{max} as effective shear strain are compared with the seismic response evaluated by GeoELSE, which updates the modulus degradation at each time step, on the basis of the actual γ_{max} averaged on each element (see section 1).

Although the numerical and analytical seismic responses are in reasonable agreement (figures 2.11 and 2.12), the differences are amplified with respect to the previous case (amplitude of 1 mm), due to a significant non-linear behaviour. The analytical results obtained using γ_{eff}= γ_{max} are damper with respect to those evaluated using γ_{eff} =0.5 γ_{max}. In this case, the numerical method amplifies both the low (< 0.3 Hz) and the high (> 1.8 Hz) frequencies with respect to the analytical one, due to the high local variability in time of the damping.

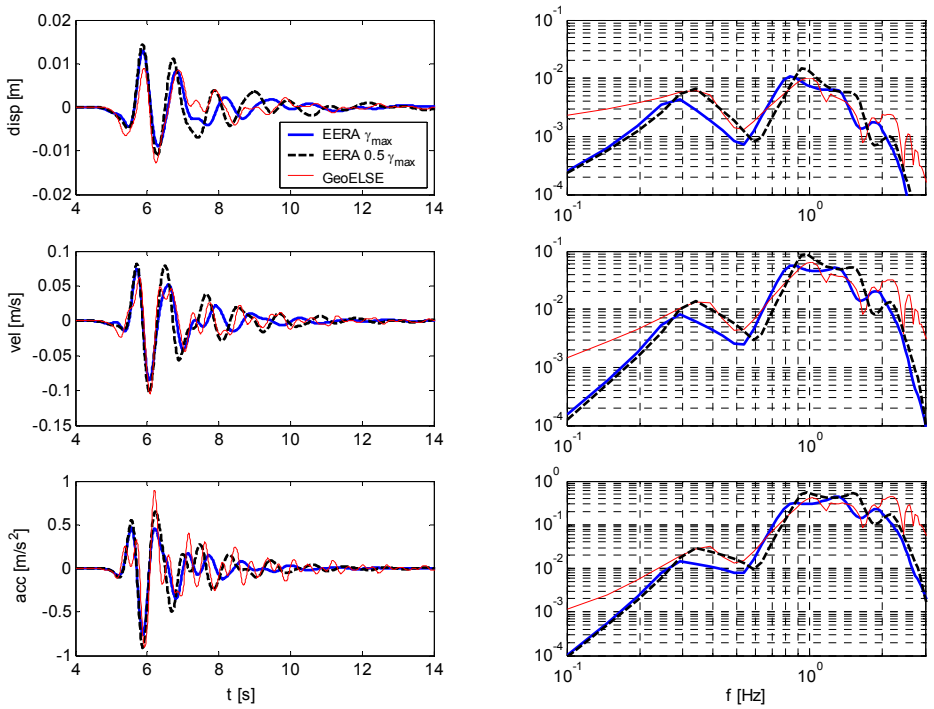

Fig. 2.11 – Comparison between the horizontal seismic responses evaluated in **non-linear viscoelastic** conditions by EERA (bold line) and GeoELSE (thin line). Time histories (left) and Fourier spectra (right) of displacement, velocity and acceleration in the horizontal direction at the representative depth of 30 m (at the middle of the layer) are shown. The seismic input is a Ricker wavelet of amplitude A= 1 cm and f_p=1 Hz, applied as vertically propagating shear wave

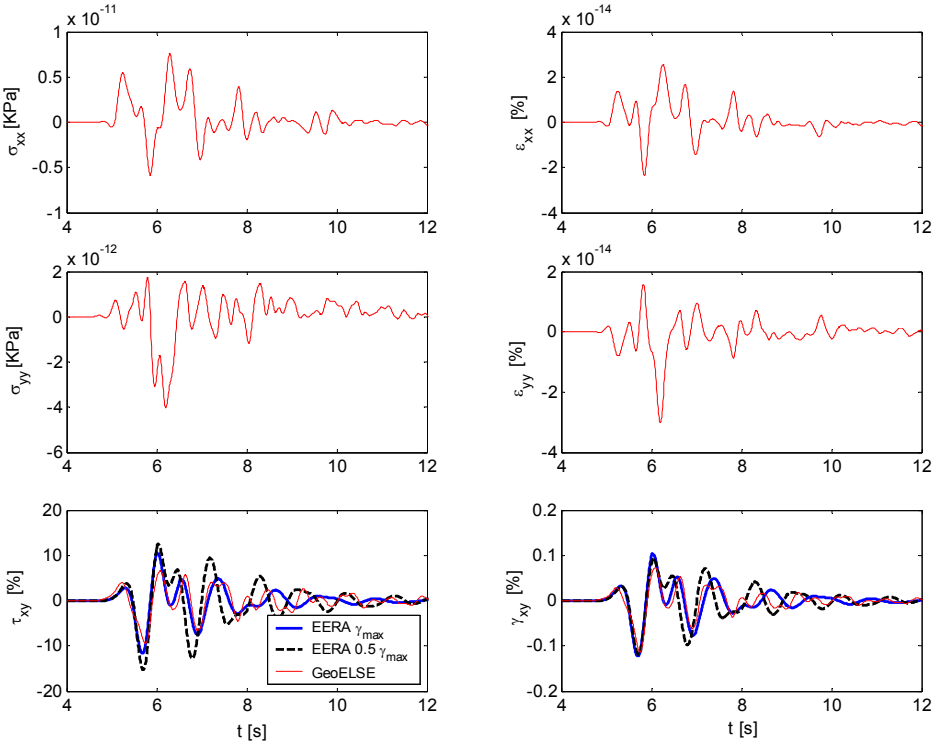

Fig. 2.12 – Comparison between the seismic responses evaluated in **non-linear viscoelastic** conditions by EERA (bold line) and GeoELSE (thin line). Time histories of stress (left) and strain (right) at the representative depth of 30 m (at the middle of the layer) are shown. The seismic input is a Ricker wavelet of amplitude A = 1 cm and f_p=1 Hz, applied as vertically propagating shear wave

The numerical G/G_0 ratio correctly follows the stress-strain curve, as shown in figure 2.13b, reaching minimum values around 0.4 between 5.8 and 6.2 sec, when the higher peaks of the signal occur (figure 2.13a). The constant analytical modulus reduction of 0.48, obtained using γ_{max}, corresponds to an average of the numerical values assumed during the passage of the most energetic part of the signal. Using 0.5 γ_{max}, a constant G/G_0 of 0.64 is applied, an average of the numerical values assumed during the passage of the signal between 5 and 10 sec.

Figure 2.14 shows that the hysteretic-stress-strain cycles obtained by the equivalent linear analysis are larger than those calculated by GeoELSE, meaning more energy dissipation. While the analytical cycles became larger in time, but with the same inclination, the numerical ones are more inclined at the beginning and became less inclined in time, meaning a gradually decrease of stiffness, due to the time updating of the modulus reduction. The loss of stiffness evaluated by the numerical method is in agreement with the stiffness obtained by EERA using γ_{max}, while using 0.5 γ_{max} EERA maintains the initial linear stiffness.

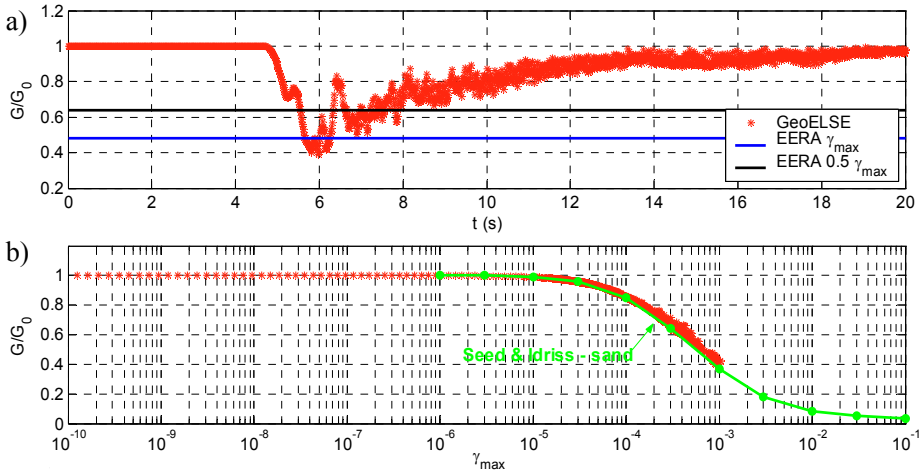

Fig. 2.13 – Seismic response calculated in **non-linear viscoelastic** conditions by GeoELSE (stars) and EERA (lines) at the representative depth of 30 m (in the middle of the layer): a) G/G_o vs. time; b) G/G_o vs. γ_{max}. The seismic input is a Ricker wavelet of amplitude A= 1 cm and f_p=1 Hz, applied as vertically propagating shear wave

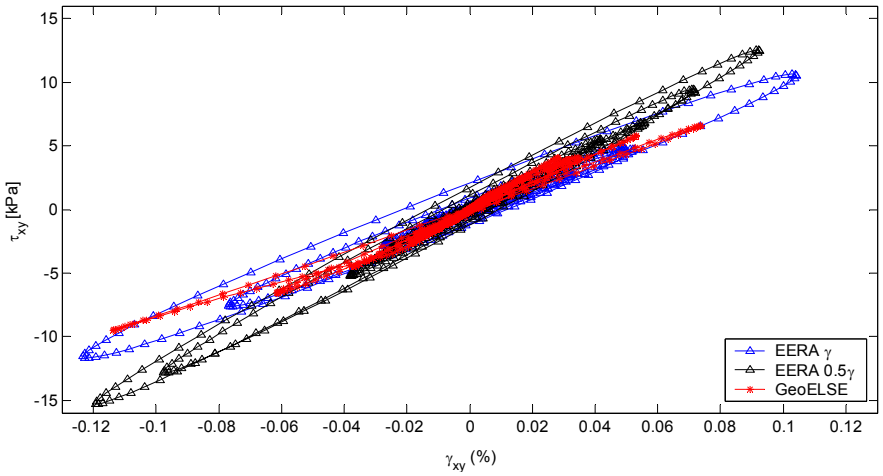

Fig. 2.14 – Comparison between the hysteretic stress-stain cycles evaluated in **non-linear viscoelastic** conditions by EERA (triangles) and GeoELSE (stars) at the representative depth of 30 m (in the middle of the layer). The seismic input is a Ricker wavelet of amplitude A= 1 cm and f_p=1 Hz, applied as vertically propagating shear wave

It is interesting to compare the amplification functions of the model both in linear and non-linear field. As shown in figure 2.15, in non-linear field the frequency peaks decrease and shift to lower frequencies. The frequency peaks obtained by the two approaches are in good agreement, except at high frequencies for 1 cm of amplitude, probably due to the not enough mesh refinement in non-linear field (see section 3.5). The numerical functions are damper with respect to the analytical ones, and the divergence obtained at frequencies closed to zero is due to numerical errors. In non-linear field, the analytical functions obtained using γ_{max} to define the modulus reduction are shift to lower frequencies and damped with respect to those obtained using $0.5\gamma_{max}$, meaning more pronounced non linear behaviour.

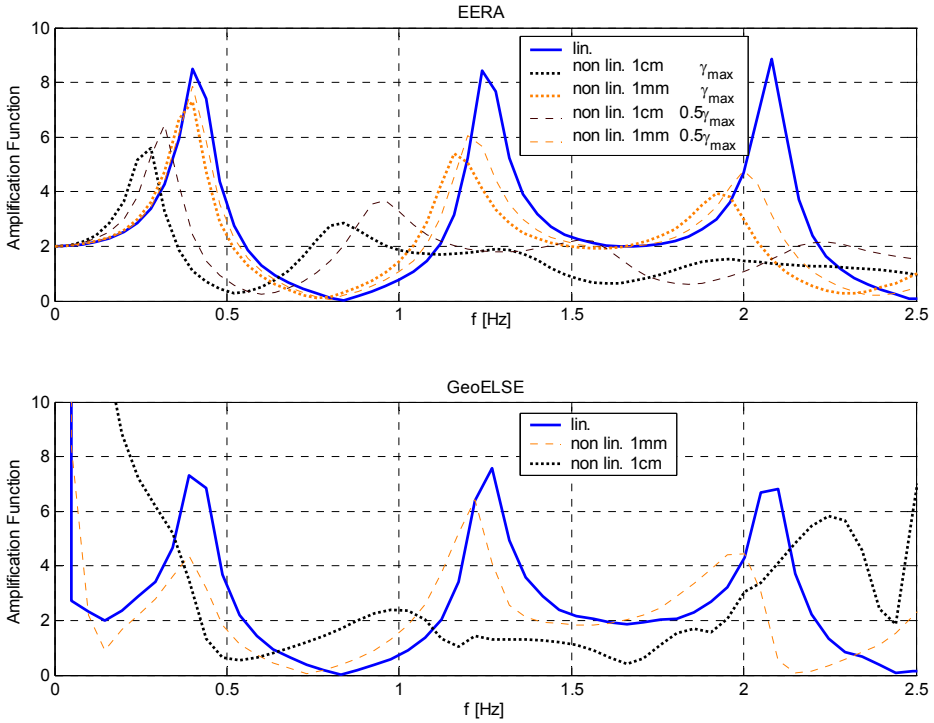

Fig. 2.15 – Comparison of the Amplification Functions evaluated in **linear** (bold lines) and **non-linear viscoelastic** (dotted lines) conditions by EERA (top) and GeoELSE (bottom) at the representative depth of 30 m (at the middle of the layer). The seismic input is a Ricker wavelet of amplitude A = 1 cm and A = 1 mm, and f_p=1 Hz, applied as vertically propagating shear wave

2.5 Comparison between SE (by GeoELSE) and FE (by CESAR-LCPC) results

The non-linear viscoelastic model implemented in GeoELSE has been also validated comparing the results whit those evaluated by the Finite Element code CESAR-LCPC (2006) by Delepine (2007).

The seismic response of a homogeneous halfspace (V_S = 200 m/s) due to a Ricker wavelet with 3 Hz of peak frequency and 0.1 g of amplitude, applied as input shear wave at 70 m depth, has been evaluated.

The assumed modulus reduction and damping-strain curves follow the relations (Delepine, 2007):

$$G(|\gamma|) = \frac{G_0}{1+\alpha_{NL}|\gamma|}$$
$$\zeta(|\gamma|) = 1 + \frac{\beta_{max}-\beta_0}{\beta_0}\left(\frac{\alpha_{NL}|\gamma|}{1+\alpha_{NL}|\gamma|}\right) \quad (2.1)$$

and they are shown in figure 2.16.

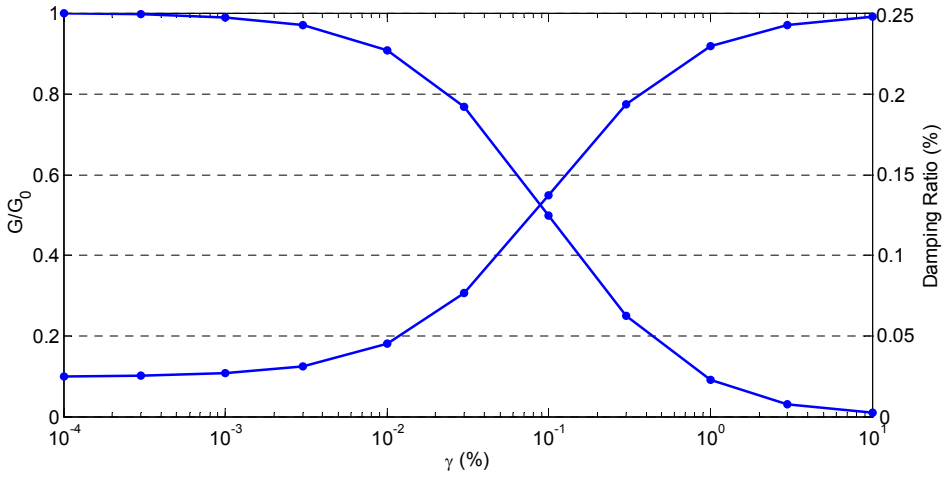

Fig. 2.16 – Stress-strain and a damping-strain curves following equations 2.1 (adopted by Delepine, 2007)

The acceleration seismic response obtained with the two approaches is shown in figures 2.17 and 2.18 respectively.

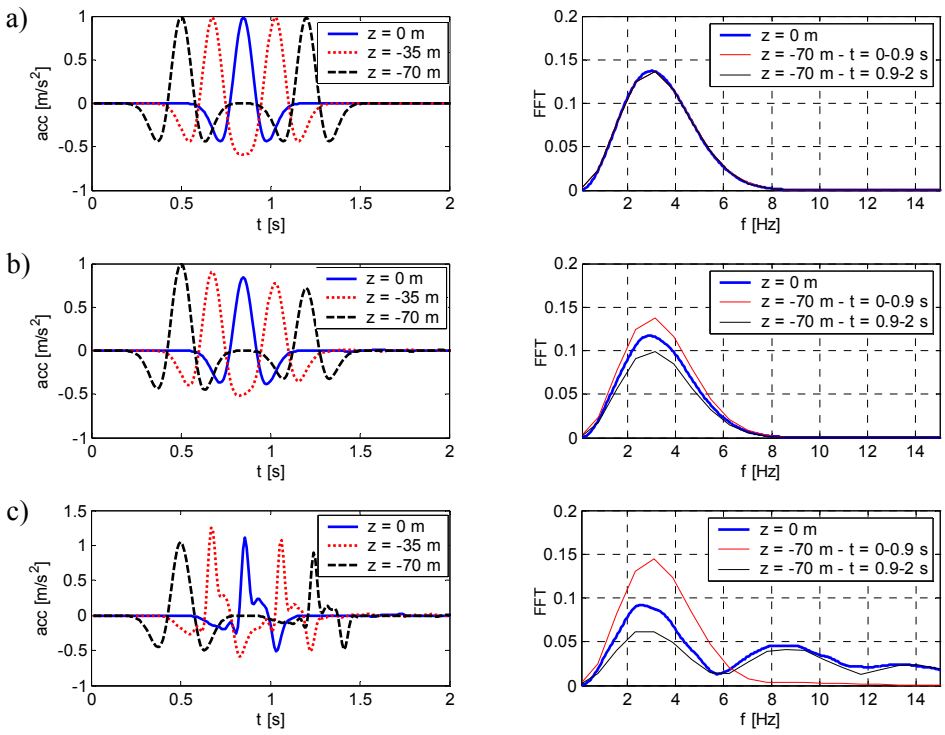

Fig. 2.17 – Spectral Element results by GeoELSE in terms of acceleration time histories (left) and Fourier Spctra (right): a) linear elastic analysis; b) linear viscoelastic analysis: Q = 20 at f_p =3 Hz; c) non linear viscoelastic analysis

The results are in good agreement. Note that, concerning the linear viscoelastic behaviour (b), the damping is different in the two approaches: a quasi-constant quality factor in CESAR-LCPC, a frequency dependent quality factor in GeoELSE:

$$Q = \frac{1}{2\zeta} \quad \text{CESAR-LCPC} \quad \text{(Delepine, 2007)}$$
$$Q = \frac{2\pi f}{2\zeta} \quad \text{GeoELSE} \quad . \tag{2.2}$$

In non-linear field, both the methods predict a spectral content characterized by not only the peak frequency of the input signal (3 Hz), but also by the higher harmonics, generated during the non-linear propagation (Delepine, 2007, Van Den Abele et al., 2000).

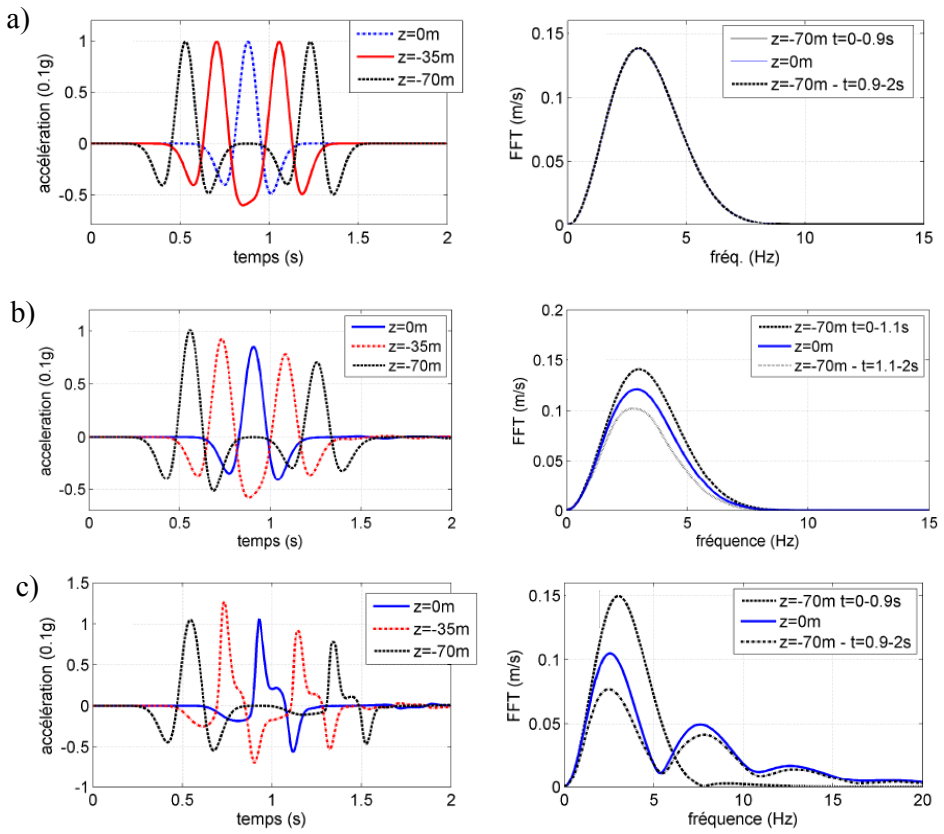

Fig. 2.18 – Finite element results by CESAR-LCPC in terms of acceleration time histories (left) and Fourier Spctra (right): a) linear elastic analysis; b) linear viscoelastic analysis: Q = 20; c) non linear viscoelastic analysis (from Delepine, 2007)

The comparison in terms of hysteretic stress-strain behaviour is shown in figure 2.19. Although the maxima stresses and strains obtained with GeoELSE are slightly smaller than those evaluated by the FE method, the responses in linear field are in good agreement. In linear viscoelastic and non-linear viscoelastic fields the FE method dissipates more energy that the SE one; in fact, while the inclination of the hysteretic cycles obtained by the two methods are in agreement, the cycles evaluated by the FE method are larger. Moreover, while stresses and strains obtained by GeoELSE are higher at 35 m depth, those obtained by CESAR-LCPC are higher at 70 m depth.

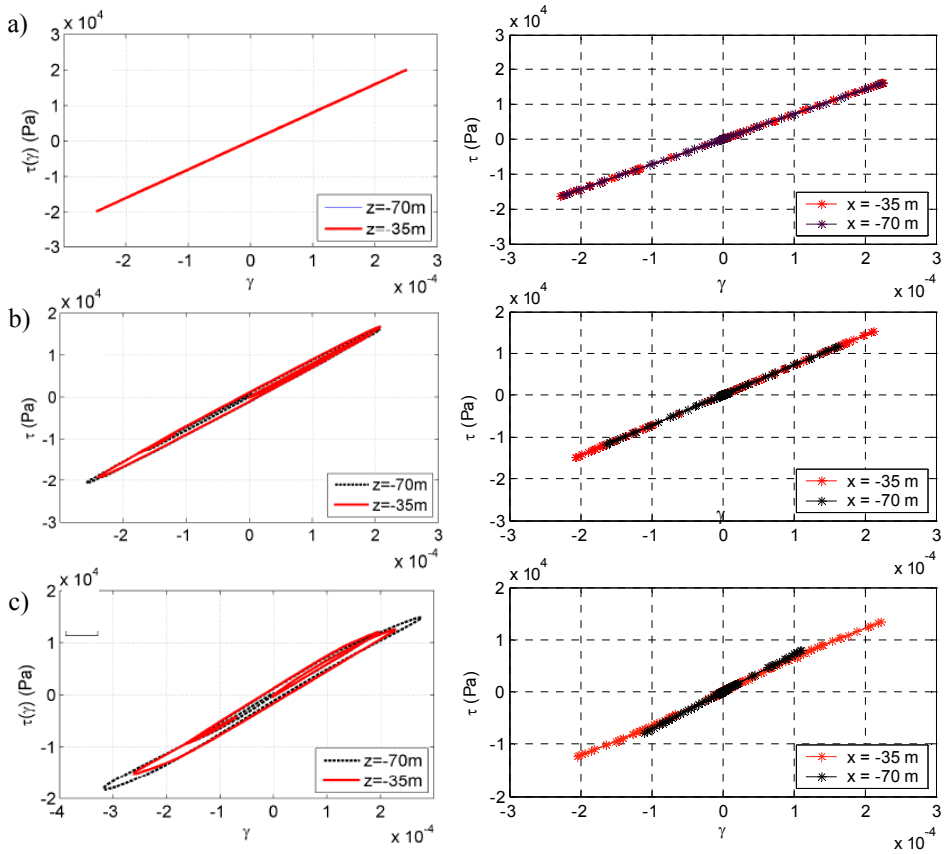

Fig. 2.19 – Comparison between CESAR-LCPC (left, from Delepine, 2007) and GeoELSE (right) results in terms of hysteretic cycles: a) linear elastic analysis; b) linear viscoelastic analysis: Q = 20; c) non linear viscoelastic analysis

3 Non-linear response due to shear wave propagation simulated by GeoELSE

Various analyses have been performed using the same 1D model described in section 2.1, varying the amplitude and the peak frequency of the Riker wavelet applied as vertically propagating shear wave. The layer has been assumed to follow the Seed & Idriss (1970) curves for sand (figure 1.2).

3.1 Variability with the seismic input amplitude

The seismic response at 30 m depth has been evaluated varying the amplitude of the Ricker wavelet from 0.1 mm to 10 cm, with a fixed peak frequency of 1 Hz (figure 3.1).

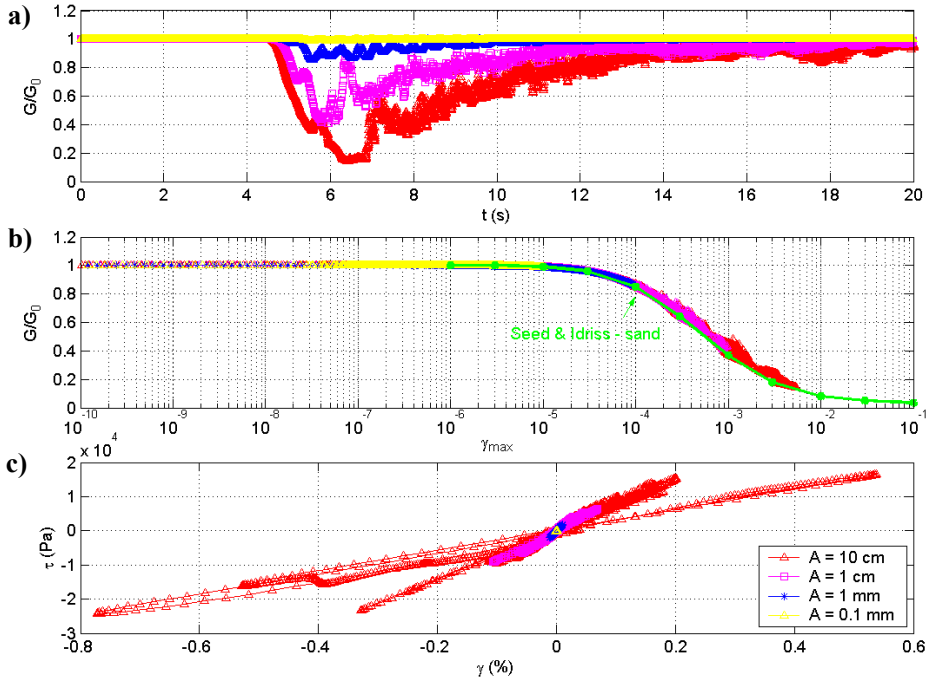

Fig. 3.1 – Comparison between the seismic responses evaluated in **linear viscoelastic** conditions by GeoELSE at the representative depth of 30 m (in the middle of the layer): (a) G/G_o vs. time; (b) G/G_o vs. γ_{max}; (c) hysteretic stress-stain cycles. The seismic input is a Ricker wavelet of amplitude A ranging from 0.1 mm to 10 cm and f_p=1 Hz, applied as vertically propagating shear wave

As expected, the non-linear behaviour becomes more pronounced increasing the Ricker amplitude: G/G_0 ratio decreases in correspondence of the signal passage (figure 3.1a); the value of the maximum shear strain γ_{max} increases (figure 3.1b) and the hysteretic cycles became larger and more inclined with time (figure 3.1c).

3.2 Variability with the seismic input frequency

The seismic response at 30 m depth has been evaluated varying the peak frequency of the Ricker wavelet from 0.2 Hz to 1 Hz, with fixed amplitude of 1 cm.

The non-linear behaviour is particularly highlighted applying a Ricker wavelet with 0.417 Hz of peak frequency, which corresponds to the resonance frequency of the layer (figure 3.2).

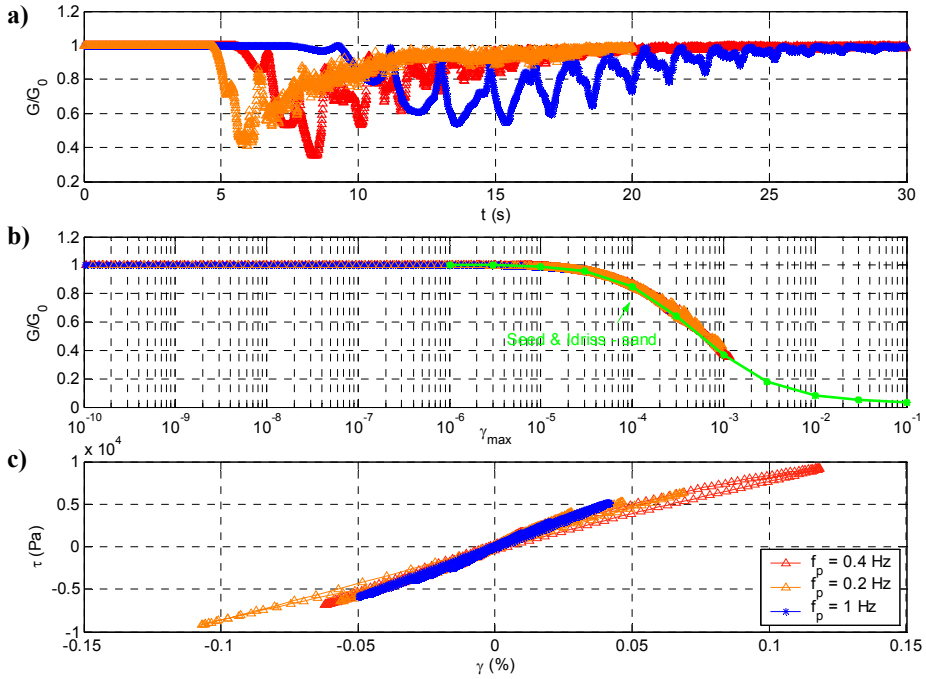

Fig. 3.2 – Comparison between the seismic responses evaluated in **linear viscoelastic** conditions by GeoELSE at the representative depth of 30 m (in the middle of the layer): (a) G/G_o vs. time; (b) G/G_o vs. γ_{max}; (c) hysteretic stress-stain cycles. The seismic input is a Ricker wavelet of amplitude A= 1 cm and f_p ranging from 0.4 Hz to 1 Hz, applied as vertically propagating shear wave

3.3 Variability with depth

The seismic response at various depths, from the surface to 60 m depth, has been evaluated applying a Ricker wavelet with fixed amplitude of 1 cm and various peak frequencies: 1 Hz (figure 3.3), 0.417 Hz (figure 3.4) and 0.2 Hz (figure 3.5).

As expected, at depth the non-linear behaviour is more pronounced with respect to the surface. Increasing the frequency content of the input signal the maximum shear strain increases and the G/G_0 ratio decreases. Note that, with f_p=0.417 Hz, being the resonant frequency of the layer, the largest hysteretic cycles and the maximum modulus degradation are obtained, in particular at 30 m depth, in the middle of the layer (figure 3.4).

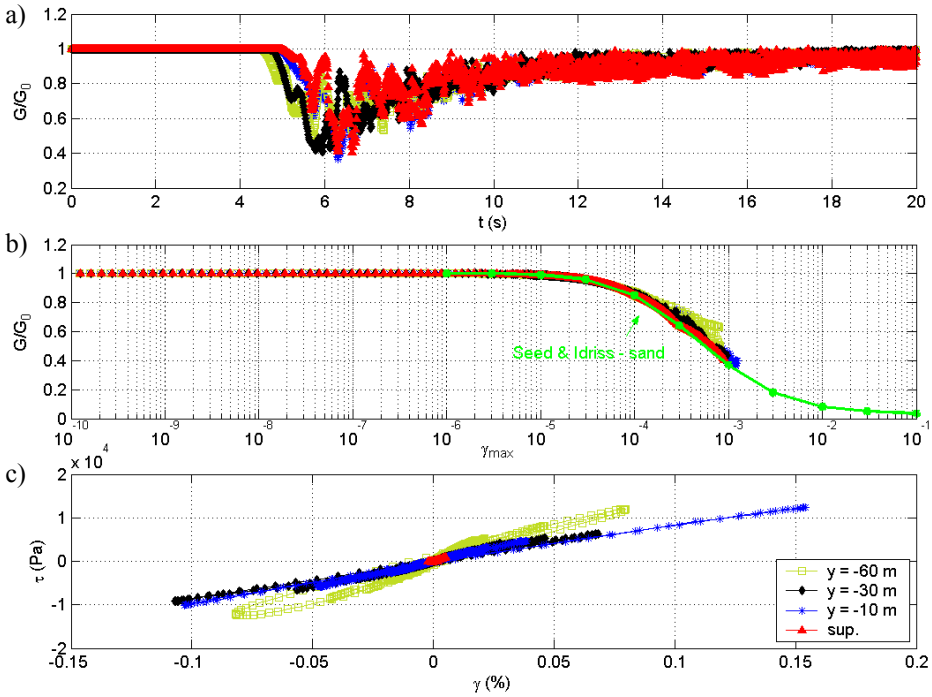

Fig. 3.3 – Comparison between the seismic responses evaluated in **linear viscoelastic** conditions by GeoELSE at various depths y, from the surface to 60 m depth: (a) G/G_o vs. time; (b) G/G_o vs. γ_{max}; (c) hysteretic stress-stain cycles. The seismic input is a Ricker wavelet of amplitude A= 1 cm and f_p **= 1 Hz**, applied as vertically propagating shear wave

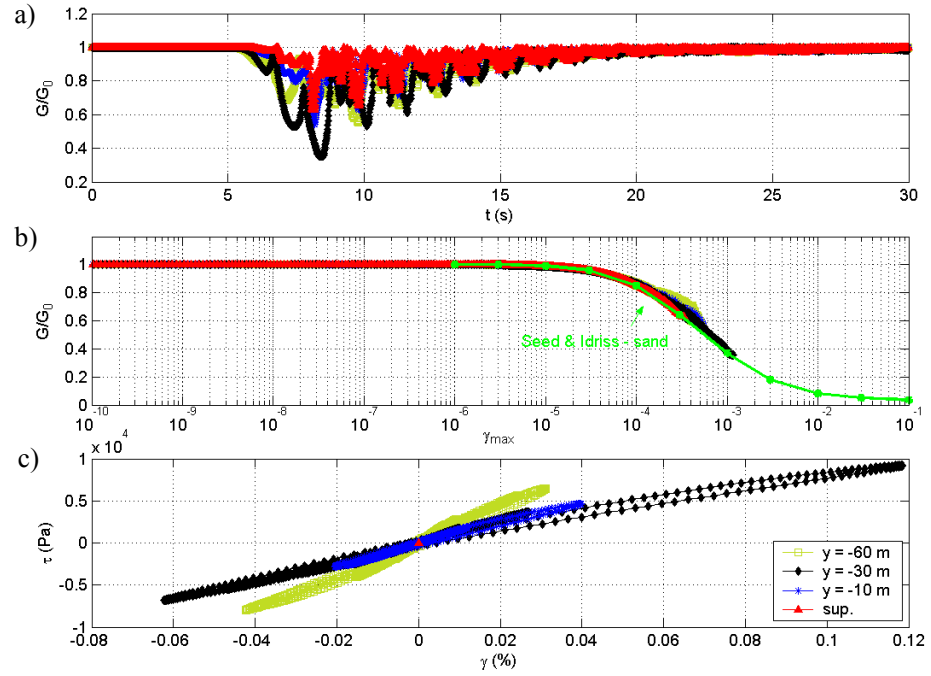

Fig. 3.4 – Comparison between the seismic responses evaluated in **linear viscoelastic** conditions by GeoELSE at various depths y, from the surface to 60 m depth: (a) G/G_o vs. time; (b) G/G_o vs. γ_{max}; (c) hysteretic stress-stain cycles. The seismic input is a Ricker wavelet of amplitude A= 1 cm and f_p **= 0.417 Hz**, applied as vertically propagating shear wave

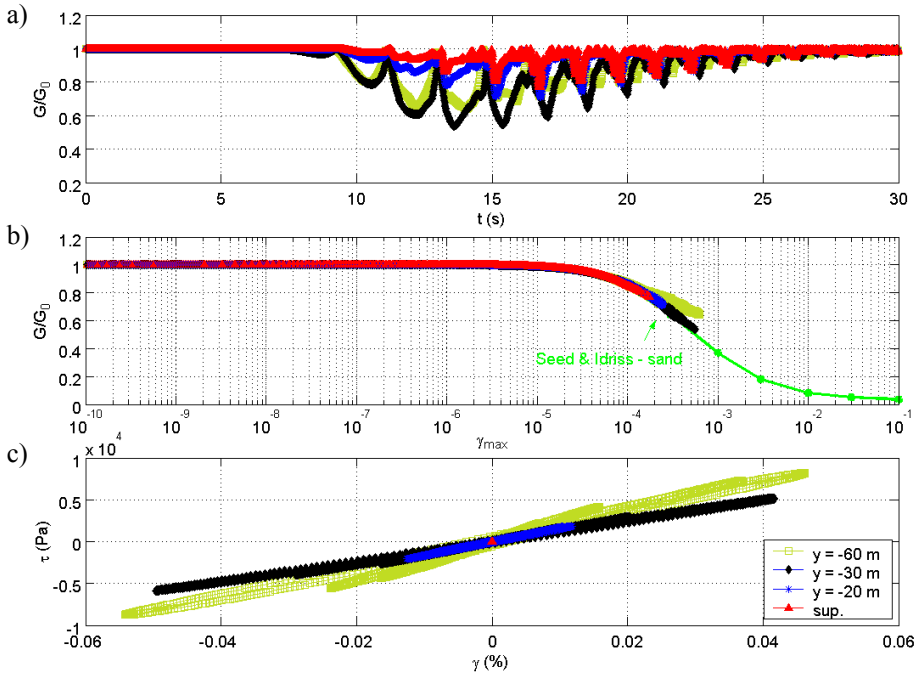

Fig. 3.5 – Comparison between the seismic responses evaluated in **linear viscoelastic** conditions by GeoELSE at various depths **y**, from the surface to 60 m depth: (a) G/G_o vs. time; (b) G/G_o vs. γ_{max}; (c) hysteretic stress-stain cycles. The seismic input is a Ricker wavelet of amplitude A= 1 cm and f_p **= 0.2 Hz**, applied as vertically propagating shear wave

3.4 Comparison between sand and clay behaviour

The seismic response at 30 m depth has been evaluated both for sand and clay, applying as input motion a Ricker wavelet with 1 cm of amplitude and 1 Hz of peak frequency.

As expected, sand shows greater non-linearity than clay. In fact sand amplifies the low frequencies (< 1 Hz) with respect to clay, while clay amplifies the high ones (> 1 Hz). Moreover, the minimum G/G_0 ratio achieved by sand is one-half that of clay (figure 3.8). Although the maximum shear strain achieved is almost the same, sand becomes less stiff, becoming the hysteretic cycles more inclined with time (figure 3.9).

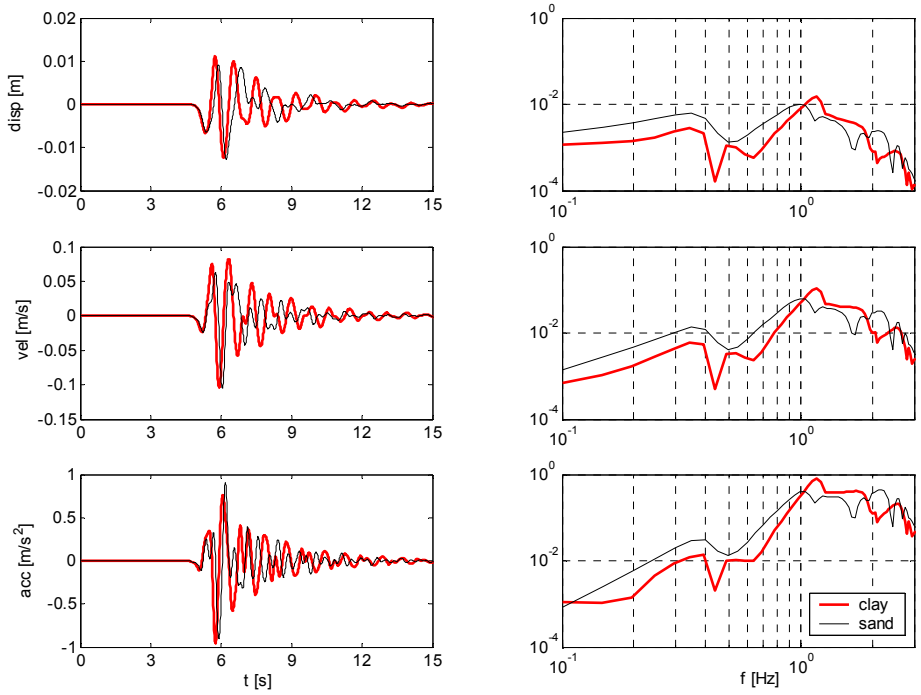

Fig. 3.6 – Comparison between the horizontal seismic responses evaluated in **non-linear viscoelastic** conditions by GeoELSE for clay (bold lines) and sand (thin lines). Time histories (left) and Fourier spectra (right) of displacement, velocity and acceleration in the horizontal direction at the representative depth of 30 m (at the middle of the layer) are shown. The seismic input is a Ricker wavelet of amplitude A= 1 cm and f_p=1 Hz, applied as vertically propagating shear wave

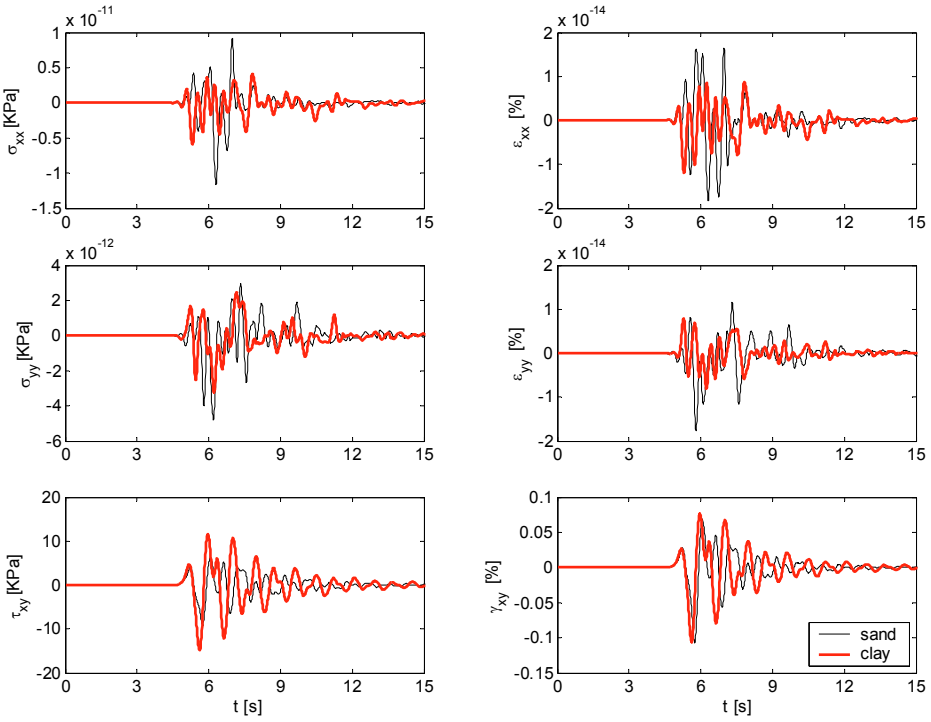

Fig. 3.7 – Comparison between the seismic responses evaluated in **non-linear viscoelastic** conditions by GeoELSE for clay (bold lines) and sand (thin lines). Time histories of stress (left) and strain (right) at the representative depth of 30 m (at the middle of the layer) are shown. The seismic input is a Ricker wavelet of amplitude A= 1 cm and f_p=1 Hz, applied as vertically propagating shear wave

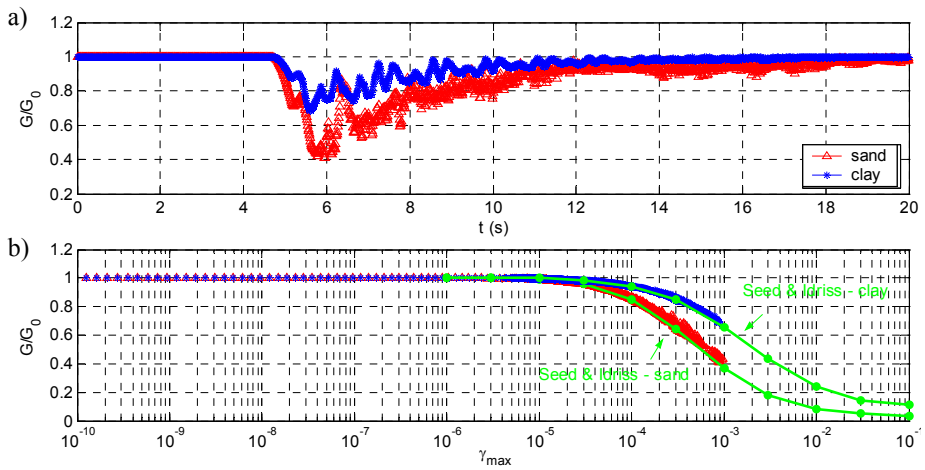

Fig. 3.8 – Comparison between the seismic responses evaluated in **non-linear viscoelastic** conditions by GeoELSE for clay (triangles) and sand (stars) at the representative depth of 30 m (in the middle of the layer): (a) G/G_o vs. time; (b) G/G_o vs. γ_{max}. The seismic input is a Ricker wavelet of amplitude A= 1 cm and f_p=1 Hz, applied as vertically propagating shear wave

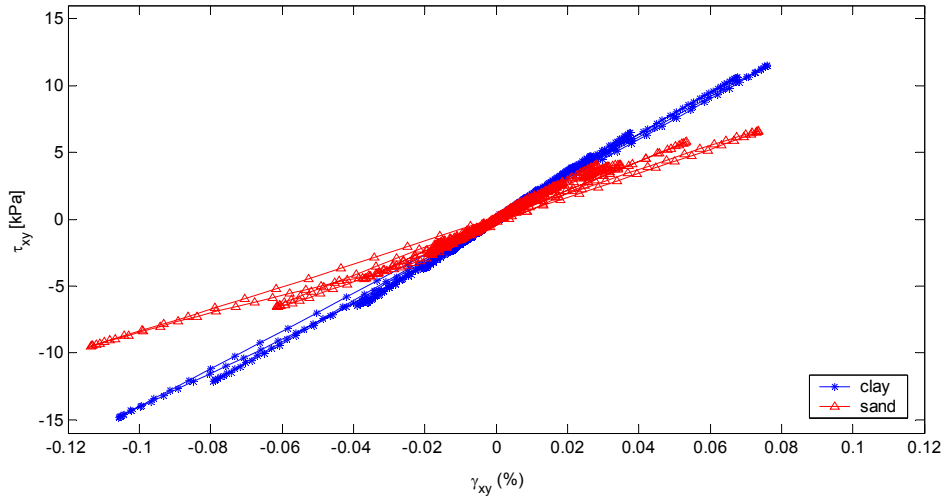

Fig. 3.9 – Comparison between the hysteretic stress-strain cycles evaluated in **non-linear viscoelastic** conditions by GeoELSE for clay (triangles) and sand (stars) at the representative depth of 30 m (in the middle of the layer). The seismic input is a Ricker wavelet of amplitude A= 1 cm and f_p=1 Hz, applied as vertically propagating shear wave

3.5 Variability on mesh refinement

The previously described numerical results have been obtained using a space discretization of 10 m for the layer, meaning an accurate propagation of wavelengths higher than 10 m, using 4 points per wavelength and frequencies up to 60 Hz:

$$\Delta x = \frac{V_S}{f_{\max}} \frac{1}{4} N = \frac{600}{60} \frac{1}{4} 4 = 10\,m\,, \tag{3.1}$$

with N the used polynomial degree. The element size is 20 times smaller (5 %) than the minimum required to propagate a Ricker wavelet of maximum frequency of 3 Hz (Δx=200 m). This is true in linear field, but in non-linear field the minimum propagation velocity is updated in time, depending on the modulus degradation (eq. 1.7). For instance, for a Ricker wavelet of 1 cm of amplitude, G/G_0 reaches minimum values of 0.4 (figure 2.13), so that the shear velocity becomes 96 m/s, requiring Δx of 32 m to propagate up to 3 Hz. Since during the numerical simulation the modulus degradation and the damping ratio may vary depending on the mesh size, the effects of the grid refinement are analysed in the following. In figure 3.10 three SE meshes of the layer at different refinement are shown.

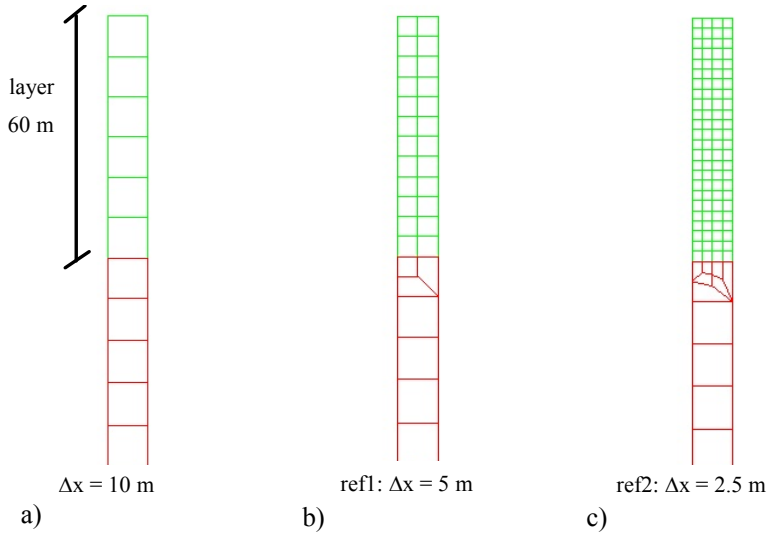

Fig. 3.10 – Spectral element grids of the 1D model of figure 2.1 with increasing spatial discretization refinement: a) Δx=10 m, b) Δx=5 m, c)) Δx=2.5 m

The comparison of the seismic responses at 30 m depth, due to a Ricker wavelet of 1 cm of amplitude and 1 Hz of peak frequency, using different mesh refinements of the numerical model is shown in figures 3.11 and 3.12. Refining the mesh the peak amplitudes decrease, especially at high frequencies (> 2.5 Hz). This is confirmed also by the amplification functions shown in figure 3.13, where the response due to a Ricker wavelet of 1 cm of amplitude improves at frequencies higher than 2 Hz.

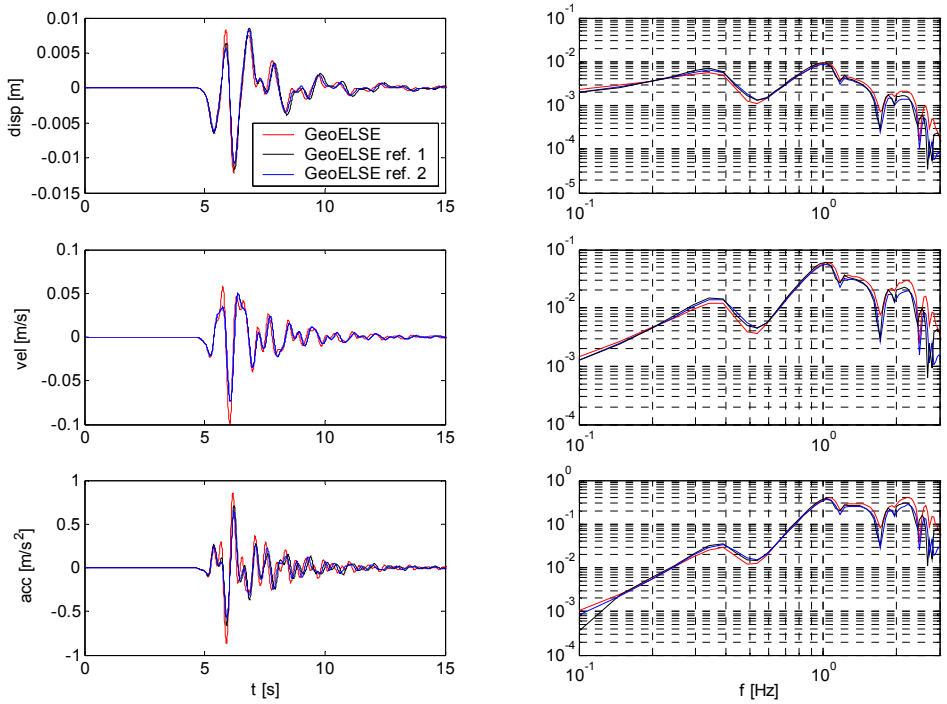

Fig. 3.11 – Comparison between the seismic responses evaluated in **non-linear viscoelastic** conditions by GeoELSE using the mesh refinements of figure 3.10 a) red thin line; b) ref1 – black thin line; c) ref2 – blue thin line. Time histories (left) and Fourier spectra (right) of displacement, velocity and acceleration in the horizontal direction at the representative depth of 30 m (at the middle of the layer) are shown. The seismic input is a Ricker wavelet of amplitude A= 1 cm and f_p=1 Hz, applied as vertically propagating shear wave

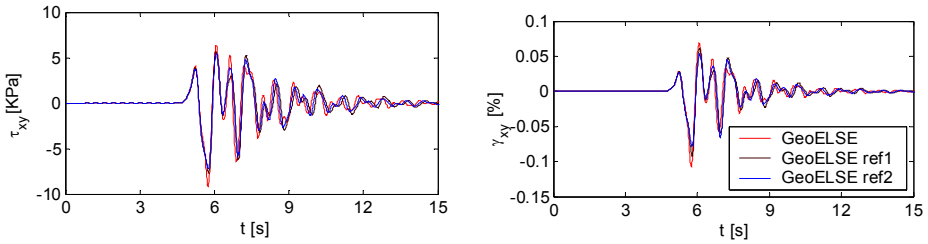

Fig. 3.12 – Comparison between the seismic responses evaluated in **non-linear viscoelastic** conditions by GeoELSE using the mesh refinements of figure 3.10 a) red thin line; b) ref1 – black thin line; c) ref2 – blue thin line. Time histories of stress (left) and strain (right) at the representative depth of 30 m (at the middle of the layer) are shown. The seismic input is a Ricker wavelet of amplitude A= 1 cm and f_p=1 Hz, applied as vertically propagating shear wave

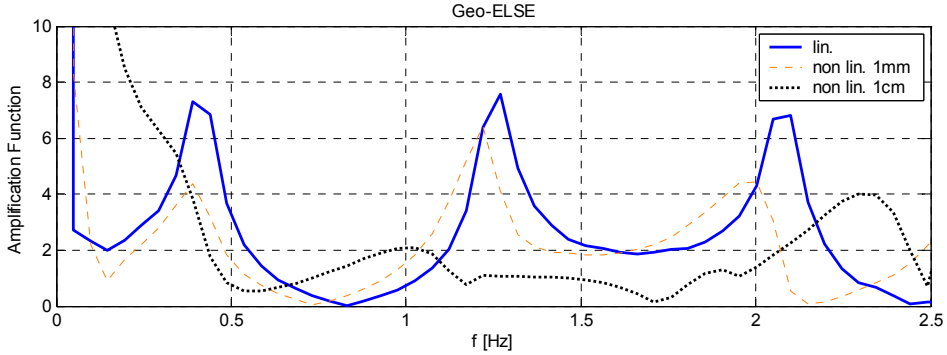

Fig. 3.13 – Comparison of the Amplification Functions evaluated in **linear** (bold line) and **non-linear viscoelastic** (dotted lines) conditions by GeoELSE at the representative depth of 30 m (at the middle of the layer). The seismic input is a Ricker wavelet of amplitude A = 1 cm and f_p=1 Hz, applied as vertically propagating shear wave. The refined mesh c) of figure 3.10 is used

The shear modulus degradation in time slightly varies with the mesh refinement (figure 3.14), while the hysteretic cycles are significantly influenced (figure 3.15). In particular, the energy dissipation increases with the loos of stiffness refining the mesh.

An exact indication about the correct space discretization in non-linear field is not straightforward to give, depending on the shear modulus degradation during the analysis.

It should be proper to perform a first analysis using the discretization required in linear field in order to evaluate the minimum G/G_0 achieved. Afterwards, on the basis of the minimum Vs evaluated, the correct Δx may be recalibrated. Otherwise, since the modulus degradation can reasonably reach at most minimum values of 0.4, it comes out from the previous analysis that a spatial discretization of 15-20% of that required in linear field may be enough to have accurate results. Note that, to have better indications, further investigations are necessary, involving real seismic inputs and different frequency ranges.

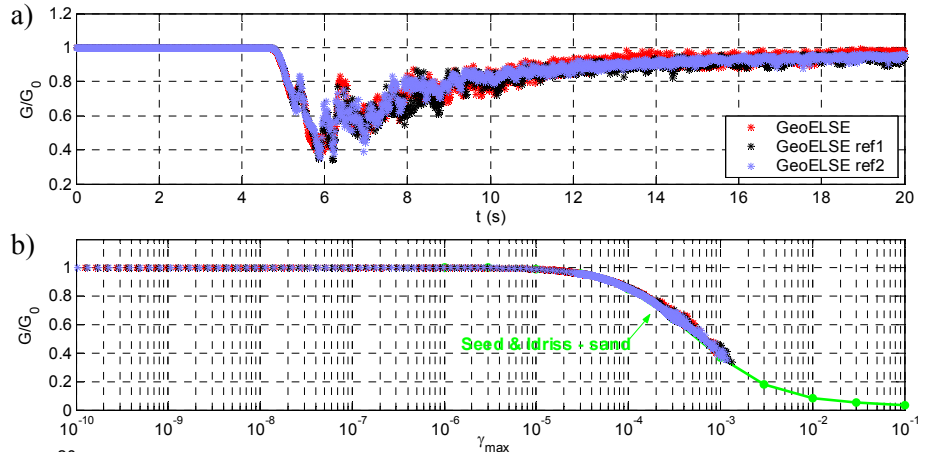

Fig. 3.14 – Comparison between the seismic responses evaluated in **non-linear viscoelastic** conditions by GeoELSE at the representative depth of 30 m (in the middle of the layer) using the mesh refinements of figure 3.10 (a) red thin line; (b) ref1 – black thin line; (c) ref2 – blue thin line: a) G/G_o vs. time; b) G/G_o vs. γ_{max}. time. The seismic input is a Ricker wavelet of amplitude A= 1 cm and f_p=1 Hz, applied as vertically propagating shear wave

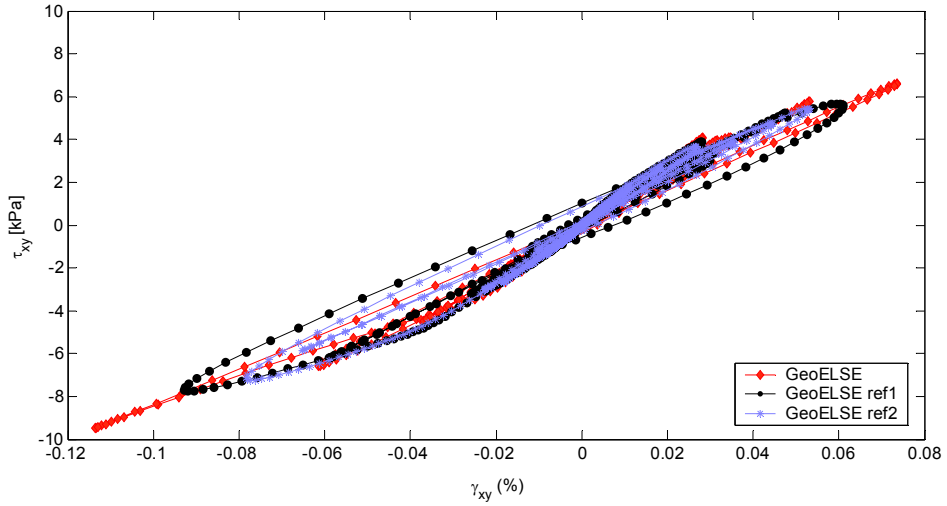

Fig. 3.15 – Comparison between the the hysteretic stress-stain cycles obtained in **non-linear viscoelastic** conditions by GeoELSE at the representative depth of 30 m (in the middle of the layer) using the mesh refinements of figure 3.10 (a) red thin line; (b) ref1 – black thin line; (c) ref2 – blue thin line. The seismic input is a Ricker wavelet of amplitude A= 1 cm and f_p=1 Hz, applied as vertically propagating shear wave

REFERENCES

CESAR-LCPC (Laboratoire Central des Ponts et Chaussées) (2006), Software solution for Geotechnical, Tunnel and Structural analysis, http://www.cesar-lcpc.com/.

Delepine N., (2007), " Modélisation des effects de site sismiques dans les bassins sédimanetaires et influence des non-linéarité de comportement des sols", Ph.D thesis, Ecole nationale des Ponts et Chaussees, Paris.

EERA (Equivalent–linear Earthquake site Response Analyses) code, (2000), http://gees.usc.edu/GEES/Software/EERA2000/Default.htm.

Idriss I.M., (1990), "Response of soft soil sites during earthquakes", Proceedings of the Symposium to Honor Professor H.B.Seed, Berkeley, CA, 273-289.

Seed H.B. & Idriss I.M., (1970), "Soil moduli and damping factors for dynamic response analyses", Report n. UCB/EERC-70/10, Earthquake Engineering Reserce centre, University of California, Barkley, California.

Van Den Abeele K., Johnson P.A., Sutin A., (2000), „Nonlinear Elstic Wave Spectroscopy (NEWS) techniques to discern material damage. Part I: Nonlinear Wave Modulation Spectroscopy (NWMS). Res. Nondestr. Eva. 12/1, 17-30, Springer-Verlag New York Inc."